



HAL
open science

The role and characterization of phospholipase A1 in mediating lysophosphatidylcholine synthesis in *Trypanosoma brucei*

Gregory S Richmond, Terry K Smith

► **To cite this version:**

Gregory S Richmond, Terry K Smith. The role and characterization of phospholipase A1 in mediating lysophosphatidylcholine synthesis in *Trypanosoma brucei*. *Biochemical Journal*, 2007, 405 (2), pp.319-329. 10.1042/BJ20070193 . hal-00478753

HAL Id: hal-00478753

<https://hal.science/hal-00478753>

Submitted on 30 Apr 2010

HAL is a multi-disciplinary open access archive for the deposit and dissemination of scientific research documents, whether they are published or not. The documents may come from teaching and research institutions in France or abroad, or from public or private research centers.

L'archive ouverte pluridisciplinaire **HAL**, est destinée au dépôt et à la diffusion de documents scientifiques de niveau recherche, publiés ou non, émanant des établissements d'enseignement et de recherche français ou étrangers, des laboratoires publics ou privés.

The role and characterization of phospholipase A₁ in mediating lysophosphatidylcholine synthesis in *Trypanosoma brucei*

Gregory S. RICHMOND¹ and Terry K. SMITH²

Wellcome Trust Biocentre, Division of Biological Chemistry and Molecular Microbiology,
College of Life Sciences, University of Dundee, Scotland, DD1 5EH

¹ Present address: Department of Microbiology, Immunology, and Molecular Genetics,
University of California, Los Angeles, CA 90095.

² To whom correspondence should be addressed:

Telephone: (44)01382 388688; Fax: (44) 01382 345764; E-Mail: t.k.smith@dundee.ac.uk

Running title: lysoGPCCho synthesis in *T. brucei*

Keywords: lysophosphatidylcholine, phospholipase, lipid metabolism, *Trypanosoma brucei*,
interfacial activation

Abbreviations used: GPCCho, (glycero)phosphatidylcholine; PL, phospholipid; FA, fatty acid;
TbPLA₁, *Trypanosoma brucei* phospholipase A₁; PCF, procyclic form; BSF, bloodstream
form; EA, enzyme-aggregate; TX-100, Triton X-100; [M+H]⁺, mass plus hydrogen positive
ion.

SYNOPSIS

Lysophospholipids are ubiquitous intermediates in a variety of metabolic and signalling pathways in eukaryotic cells. We have recently reported that lysophosphatidylcholine (lysoGPCho) synthesis in the insect form of the ancient eukaryote *Trypanosoma brucei* is mediated by a novel phospholipase A₁ (TbPLA₁). In this report it is shown that despite equal levels of *TbPLA₁* gene expression in wild type insect and bloodstream trypomastigotes, both TbPLA₁ enzyme levels and lysoGPCho metabolites are approximately three fold higher in the bloodstream form. Both of these parasite stages synthesize identical molecular species of lysoGPCho. *TbPLA₁* null mutants in the bloodstream form of the parasite are viable but are deficient in lysoGPCho synthesis, a defect which can be overcome by the expression of an ectopic copy of *TbPLA₁*. The biochemical attributes of TbPLA₁-mediated lysoGPCho synthesis were examined *in vitro* using recombinant TbPLA₁. Although TbPLA₁ possesses a serine active site residue, it is insensitive to serine-modifying reagents such as DFP and PMSF, a characteristic shared by lipases that possess lid-sheltered catalytic triads. TbPLA₁ needs no metal co-factors for activity but it does require interfacial activation prior to catalysis. Results from size exclusion chromatography and binding kinetics analysis revealed that TbPLA₁ activation by Triton X-100/GPCho mixed micelle surfaces was not specific and did not require the pre-formation of a specific enzyme-substrate complex to achieve surface binding.

INTRODUCTION

All eukaryotic organisms are thought to metabolize phospholipids (PLs) by expressing a highly regulated and variable complement of the phospholipases A₁, A₂, C, D, and B. In *Trypanosoma brucei*, a medically important protist that causes African sleeping sickness, the complement of cellular phospholipases has not been fully elucidated. The only identified phospholipase in *T. brucei* was GPI-PLC, which specifically recognizes glycosylphosphatidylinositol (GPI) membrane anchors [1-3]. However, a highly active PLA₁ has recently been cloned in *T. brucei* [4]. TbPLA₁ exhibits substrate preference towards phosphatidylcholine (GPCho) and produces unsaturated lysoGPCho metabolites *in vivo*, about 50% of which contain a long and highly unsaturated fatty acid (FA) chain of 22 carbons [4]. Bacteria secrete PLA₁ [5, 6] but TbPLA₁, which has a bacterial origin, is localized to the cytosol of *T. brucei* [4]. In the insect procyclic form (PCF) of *T. brucei* TbPLA₁-synthesized lysoGPCho metabolites have homeostatic levels of approximately 156 pmol/10⁸ cells [4].

LysoGPCho is an amphiphilic lipid metabolite derived from GPCho, whose levels are vitally managed by balancing synthesis with degradation. Like in other eukaryotes, GPCho is the most abundant PL in *T. brucei*, comprising about 57% and 48% of total cellular PL in PCF and mammalian bloodstream form (BSF), respectively [7, 8]. Unlike in other eukaryotes, however, how *T. brucei* cells regulate GPCho homeostasis is not understood. In the higher eukaryotes GPCho is metabolized by one of a number of lipolytic reactions, the best characterized ones being the following: 1) saturated lysoGPCho is synthesized by a phospholipase A₂ (PLA₂), of which one type deacylates GPCho-derived arachidonic acid for use in cell signalling [9]; or 2) saturated lysoGPCho is synthesized by the action of lecithin-cholesterol acyltransferase (LCAT) [10]; or 3) phospholipase D (PLD) catalyzes the hydrolysis of GPCho to phosphatidic acid and choline [11]; or 4) phospholipase B (PLB) deacylates the fatty acyl moieties of GPCho to form glycerophosphocholine and free FAs [12-14], a degradation pathway which is stimulated by Sec14 [15, 16]. Interestingly, *T. brucei* is thought to lack PLA₂ activity [17] and analysis of its genome does not reveal putative PLA₂ or PLD homologues [4]. On the other hand, several lysophospholipase (LysoPLA)/PLB homologues are present in the database, which may explain previous reports that observed their corresponding specific esterase activity [18-21]. Despite the possession of an LCAT homologue in *T. brucei*, this parasite contains minute quantities of saturated lysoGPCho

species and synthesizes instead mostly polyunsaturated and highly unsaturated lysoGPCho by TbPLA₁ [4].

T. brucei spends much of its life in the mammalian systemic circulation from which it acquires its nutrients, which include saturated and unsaturated lysoGPCho [18, 22]. Unsaturated lysoGPCho in mammalian plasma accounts for roughly only 1-4% of total plasma phospholipids [23] and, though formed by an undefined mechanism, is derived from hepatic secretion [24]. It was originally thought that plasma lysoGPCho acquired by the bloodstream form of *T. brucei* was detoxified by the cell's robust PLA₁ activity [18, 19, 25]. This is most likely not the case, however, since TbPLA₁ is cytosolic and metabolizes endogenous GPCho [4]. With a long-term goal to elucidate the biological significance of TbPLA₁ in *T. brucei*, we herein investigate endogenous lysoGPCho synthesis in the bloodstream form of *T. brucei* and relate this activity to its insect stage equivalent. We also further characterize TbPLA₁-mediated lysoGPCho synthesis *in vitro* in order to further understand the properties of this novel eukaryotic enzyme.

EXPERIMENTAL

Materials

Analytical reagents were bought from Sigma unless otherwise stated. Synthetic PLs were purchased from Avanti Polar Lipids, Inc. Chemicals used for bulk buffer production were from BDH unless otherwise stated. All solvents were HPLC grade and from BDH.

Generation and analysis of BSF *TbPLA₁* mutants

Deletion constructs for BSF WT transformation were synthesized by a series of amplification and cloning steps similar to that which was described in detail when the PCF *TbPLA₁* mutants were obtained [4]. Briefly, the 5'-UTR and 3'-UTR sequences of *TbPLA₁* were amplified, linked, and inserted into a cloning vector. Puromycin (*puro^R*) and hygromycin (*hyg^R*) drug resistance genes were then ligated individually between the UTR sequences which generated the deletion constructs 5'-*puro^R*-3' and 5'-*hyg^R*-3'. The over-expression vector *pLEW82/PLA1-HA* was constructed by cloning *TbPLA₁* into *pLEW82* using the same primers used to construct *pLEW100/TbPLA₁* [4].

The BSF *in vitro* culture cell line (strain 427, MITat 1.2) used throughout these studies are from the long term cultures of 'single marker' cells from Wirtz *et al.* that express a tetracycline repressor (TetR) and T7 RNA Polymerase (T7RNAP) [26], and was maintained under neomycin (G418) drug pressure at a final concentration of 2.5 µg/ml. BSF cultures were maintained below a cell density of 2×10^6 /ml in HMI-9 media at pH 7.5 which contained 10% heat-inactivated foetal bovine serum (FBS) (PAA Labs) and 10% Serum Plus (JRH Biosciences) as lipid sources. BSF transformation with DNA constructs was achieved through electroporation as previously described [4] except that the cells were left to recover in the incubator for 6-24 h in 24 ml HMI-9 before distribution and drug selection in a 12-well plate. Transformed cells containing the puromycin and/or hygromycin resistance genes were cultured in the presence of these drugs at final concentrations of 0.1 µg/ml and 4 µg/ml respectively. Drug resistant parasites appeared between 5-7 days at which time an aliquot of cells were used to start a new culture. Clonal populations of cells were obtained through limiting dilution.

BSF cell lines were analyzed by Southern and northern blotting, performed exactly as previously described [4], as was the nano-electrospray tandem mass spectrometry (ESI-MS-MS) analysis. Western blot analysis was performed on 10^7 cell equivalents/lane that were

obtained by resuspending cultured cells in boiling SDS-PAGE sample buffer at a concentration of 10^6 cells/ μ l.

Infectivity of genetically modified parasites was examined in mice (n=5 mice for each cell-line). Adult mice (BALB/c) were infected intraperitoneally with a single injection of either 5×10^5 WT *T. brucei* bloodstream trypomastigotes or 5×10^5 genetically modified *TbPLA₁* null mutants. Blood parasitaemia was monitored at 24, 48 and 72 h.

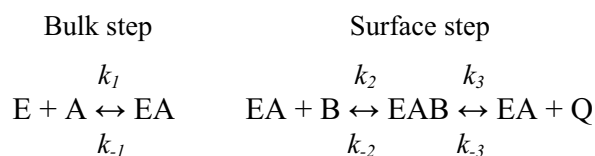
Electrospray tandem mass spectrometry

Total lipids from 10^8 mid-log BSF trypanosomes were extracted and analyzed as previously described [4]. Briefly, the resultant lower phase lipid extract from a Bligh and Dyer extraction [27] was dried under nitrogen and re-dissolved in 20 μ l of chloroform/methanol (1:2). Internal standards, lysoGPCho(17:0/-) and lysoGPCho(24:0/-) (0.5 nmol/standard), were added prior to lipid extraction. Aliquots were analyzed by nanoflow capillary ESI-MS-MS in positive ion mode for GPCho species with a Micromass Quattro Ultima triple quadrupole mass spectrometer with capillary/cone voltages and collision gas as described previously [4]. Each spectrum encompasses at least 50 repetitive scans of 4 s duration.

'Surface dilution' kinetic scheme

For clarity, the concept of 'surface dilution' kinetics is briefly explained here. Lipolytic enzymes act preferentially on substrates which are aggregated at lipid-water interfaces and this makes kinetic analysis with lipids more complicated than with simple water-soluble substrates. Interface-dependent enzymes work in an environment where bulk interactions occur three-dimensionally in solution and surface interactions occur in two dimensions, and any kinetic model for these types of enzymes must consider both types of actions in their proposed mechanism. *Deems et al* [28] proposed the 'surface dilution' kinetic model after showing that both the surface concentration of lipid and the bulk concentration of lipid in a reaction play important roles in elucidating kinetic parameters of enzymes that require interfacial activation.

The 'surface dilution' kinetic model's interfacial activation principles are expressed in the following manner:



A soluble enzyme (E) initially associates with a lipid/TX-100 mixed micelle aggregate (A) to form an enzyme-aggregate complex (EA). Once the enzyme associates with the aggregate it proceeds to bind to a substrate lipid molecule (B) in its catalytic site thus forming another complex (EAB). Products of the reaction (Q) are formed during catalysis and the EA complex is regenerated. The previous two steps are confined to the surface and so the reaction is a function of the surface concentration of the substrate and not its bulk concentration, a deviation from classic Michaelis-Menton kinetics. Due to the surface being composed of both lipid and detergent, substrate surface concentration is expressed as a unitless mole fraction, $X_s = [\text{lipid}]/[\text{lipid} + \text{detergent}]$, and it is thus possible to vary the substrate surface concentration simply by adding or subtracting detergent, hence the name ‘surface dilution’ kinetics.

The initial EA complex can be formed in two ways and ‘surface dilution’ kinetics can be applied to determine in what form EA exists. It is possible that the enzyme binds nonspecifically to the micelle surface, the ‘surface binding’ model, in which case term A is expressed as the molar concentration of both the lipid and detergent that make up the micelle [28]. Conversely, it is feasible that the enzyme could specifically bind to a lipid substrate in the micelle with one binding site, forming EA, before specifically binding at another site to another lipid molecule for catalysis, this case has been termed the ‘dual phospholipid binding’ model [29, 30]. The data analysis performed in this study used the equations derived previously and made the same assumptions necessary to ascertain kinetic parameters [28].

Bis-BODIPY[®] FL-C₁₁-PC kinetic assay

Bis-BODIPY[®] FL-C₁₁-PC (Molecular Probes) was used as a GPCho fluorescent substrate at a 1:100 molar ratio with GPCho(16:0/16:0), and TX-100/lipid micelles were made with this mixture. In its diacyl state, the proximity of the BODIPY fluorophores on adjacent PL acyl chains causes an intramolecular self-quenching of fluorescence. Hydrolysis and release of an

acyl chain by a phospholipase A alleviates quenching and an increase in fluorescence results. The fluorophores are situated at the ends of two eleven carbon chains thus mimicking a GPCho with an approximate length near to that of GPCho(16:0/16:0).

The assay was developed for use in a 96-well plate. PL and TX-100 varied according to experimental conditions and micelles were made as an 8x working solution which was then diluted accordingly for use in an 80 μ l reaction/well. Each well initially contained 40 μ l of buffer (50 mM Tris-HCl, pH 7.0) containing the desired amount of micelle substrate. The reaction was started by the addition of 40 μ l reaction buffer (50 mM Tris-HCl, 100 mM NaCl, pH 7.0) containing 400 pg (11.4 pmol) of recombinant TbPLA₁, obtained as previously described [4]. The reaction was left to proceed at 22°C for 30 min. before quenching with 170 μ l of 100% methanol. Liberated acyl chains containing a fluorophore were excited at 485 nm and detected through a 520 nm-centered bandpass filter using the FLX 800 Microplate Reader (Bio-Tek Instruments). All experiments were performed at least three times in triplicate and data points varied by less than one standard deviation. Velocities obtained were initial velocities. When the assay was used to test activity in the presence of metals and inhibitors, the variable conditions are stated in the table legends. Statistical significance was measured by applying a students paired t-test with a minimum 95% confidence interval.

Preparation of lipid/detergent mixed micelles

Manufacturer stock vials of PL were dissolved at 2.5-10 mg/ml with chloroform:methanol (1:2 v/v) and stored in the dark at -80°C until use. The desired amount of the fluorescent substrate mix was aliquoted to 1.5 ml Apex screw-cap microtubes (Alpha) and dried under nitrogen while being protected from light. The lipids were resuspended in micelle buffer heated to 40°C. The micelle buffer consisted of 50 mM Tris-HCl, pH 7.0 and the appropriate quantity of TX-100 to make the desired mole fraction. This solution was then vigorously vortexed for 1 min. and placed in a 40°C sonicator (Ultrawave Limited) until the solution cleared, with intermittent vortexing. The fluorescent mixed micelles were prepared fresh.

Gel filtration analysis

A Superdex 200 10/300 GL column (Tricorn) with an approximate bed volume of 24 ml was connected to an ÄKTA Purifier pump and equilibrated in a detergent-free buffer (50 mM Tris, 50 mM NaCl, pH 7.5) over one and a half column volumes with a flow rate of 0.5 ml/min. at 22°C. The column was calibrated with a mixture of molecular weight markers (Bio-Rad 151-1901). The markers were prepared as instructed by the manufacturer and 150 µl of the standard solution was diluted with buffer to 250 µl, loaded onto the column, separated by size exclusion and detected by UV absorbance at 280 nm. The markers and their respective molecular weights are as follows: thyroglobulin, 670 kDa; γ-globulin, 158 kDa; ovalbumin, 44 kDa; myoglobin, 17 kDa; and vitamin B₁₂, 1.35 kDa. A calibration curve was prepared by measuring the elution volumes of the standards, calculating their corresponding partition coefficient (K_{av}) values, and plotting their K_{av} values versus the logarithm of their molecular weight. K_{av} was calculated from the equation $K_{av} = (V_e - V_o) / (V_t - V_o)$, where V_e is the peak elution volume, V_o is the void volume, and V_t is the total bed volume.

Purified His-tagged recombinant TbPLA₁ (125 µl at 10 mg/ml dialyzed against buffer) and a 13.7 kDa ribonuclease A internal standard (125 µl at 3 mg/ml dissolved in buffer) were combined and loaded onto the gel filtration column. The peak elution volumes and times were used to calculate their K_{av} and the molecular weight of recombinant TbPLA₁ was determined from the calibration curve. After the last sample had eluted, the column was immediately re-equilibrated in a buffer containing TX-100 (50 mM Tris, 50 mM NaCl, 0.05% TX-100, pH 7.5), a new calibration run was performed, and another sample containing recombinant TbPLA₁ spiked with RNase A was loaded and analyzed as described.

RESULTS AND DISCUSSION

Life cycle stage expression of *TbPLA₁*

To initially examine the potential of PCF and BSF cells to synthesize lysoGPCho, an analysis of the expression of *TbPLA₁* in both these stages of the parasite life cycle was made by northern blotting. *TbPLA₁* mRNA levels are nearly equal in PCF and BSF cells (Fig. 1A). However, western blot analysis of these cells offered a different perspective since *TbPLA₁* levels in BSF cells were 3.6-fold greater than in PCF cells (Fig. 1B). These findings justified an examination into the *in vivo* activity of *TbPLA₁* in BSF cells so that lysoGPCho synthesis in PCF and BSF cells could be compared.

Construction and integrity of *TbPLA₁* mutants

Before further comparative biochemical and enzymic studies could be performed, experiments which led to the generation of a BSF double knockout of *TbPLA₁* were warranted. Deletion constructs (*5'-puro^R-3'*, *5'-hyg^R-3'*) targeted to the 5' and 3' flanking regions of the *TbPLA₁* ORF were generated and the genes for puromycin and hygromycin resistance were cloned between these flanking regions. These constructs were used to stably transform BSF parental cells that are referred to here as wild type (WT) cells, these cells are commonly used in reverse genetic studies in *T. brucei* and are transgenic clones which constitutively express T7 RNA polymerase and the tetracycline repressor protein [26]. *TbPLA₁* is a single copy gene that appears not to be essential for PCF cell viability in culture [4]. This seems also to be the case for BSF cells; two successive and successful rounds of gene replacement by UTR-targeted homologous recombination using the *5'-puro^R-3'* and *5'-hyg^R-3'* deletion constructs were sufficient to replace the two alleles of *TbPLA₁*, with no apparent resulting phenotype. Evidence for the generation of three BSF *TbPLA₁* null mutant cell lines (*Δpla1*) is shown by Southern blot analysis (Fig. 2A).

To create an additional analytical tool, a genetic transformation was also carried out that attempted to generate a cell line (*Δpla1rescPLA1-HA*) which over-expressed a rescue copy of *TbPLA₁* in a *Δpla1* background. To achieve this, a transformation was carried out using the *T. brucei* tetracycline-inducible over-expression vector *pLEW82* [31] engineered to contain a recombinant form of *TbPLA₁* (Fig. 2A). Upon tetracycline induction, trypanosomes

transformed with *pLEW82/PLA1-HA* produce an ectopic copy of TbPLA₁ with a C-terminal HA tag (PLA1-HA). The resultant tetracycline-induced *Δpla1 rescPLA1-HA* rescue clones produced *PLA1-HA* mRNA transcripts >6 fold over the level of *TbPLA₁* mRNA in both the WT and their respective uninduced counterpart cells (Fig. 2B).

The TbPLA₁ rescue cells were examined for their ability to translate their over-expressed *TbPLA₁* mRNA. A western blot probed with anti-TbPLA₁ antibodies revealed that expression of PLA1-HA was observed to be much less abundant than *TbPLA₁* mRNA in WT cells despite the high level of *PLA1-HA* mRNA over-expression (Fig. 2C). It has previously been observed that lysoGPCCho synthesis in *T. brucei* is partly regulated at the level of translation of *TbPLA₁* mRNA to control enzyme levels [4]; therefore, an over-regulation of *TbPLA₁* mRNA processing as a response to its over-expression in BSF *Δpla1 rescPLA1-HA* mutants may account for a decrease in TbPLA₁ expression. The existence of regulatory-like processes to control TbPLA₁ concentration could be significant events in the cell considering the potential harm a membrane degrading enzyme such as TbPLA₁ could foster if expressed at uncontrollable levels.

The growth rate of cultured BSF *TbPLA₁* mutants was assessed two months after creation of the *Δpla1 rescPLA1-HA* rescue cell line. *TbPLA₁* mutants are not compromised in their ability to divide and establish long-term cultures, and the population growth rate between the WT and *TbPLA₁* mutants (under drug pressure) was not significantly altered (Fig. 2D). Though *TbPLA₁* is not an essential gene in culture, it remained to be investigated whether or not, under more physiological relevant conditions, the loss of *TbPLA₁* would not be detrimental to the proper functioning of the cell. Thus, the virulence of BSF *Δpla1* cells was compared with BSF WT cells in their capacity to establish an infection in an animal model system. Analyzing the daily blood parasitaemia in inoculated mice revealed that the virulence of *Δpla1* trypanosomes was not noticeably different from the WT: high parasitaemias of $\sim 1.6 \times 10^9$ trypanosomes/ml of blood, nearly equal to that of the WT control, were reached within 72 h with an inoculum of 5×10^5 trypanosomes.

lysoGPCho analysis of *TbPLA₁* mutants

PLs are vital components of membranes and the phospholipases that modify them are recognized as important factors in mediating membrane dynamics. In PCF trypanosomes it was shown that *TbPLA₁* is a major lipolytic enzyme used by *T. brucei* to metabolize GPCho [4]. To show this, an efficient qualitative and quantitative method was employed to separate and characterize the major *T. brucei* PL classes and their molecular species from total lipid extracts using nano-electrospray tandem mass spectrometry (ESI-MS-MS). The same method was used here to analyze the choline-PL content of BSF cellular lipids by scanning for the collision-induced specific fragment ion m/z 184 (Fig. 3A). The $[M+H]^+$ GPCho molecular species composition of BSF trypomastigotes was examined and compared to that previously determined from PCF cells (compare Fig. 3A to Fig. 5A of ref. [4]). The pool of GPCho in both the PCF and BSF WT lipid extracts of *T. brucei* is comprised of the same molecular species of diacyl, alkylacyl, and alkenylacyl lipids. However, BSF *T. brucei* appear to contain more lipids in the series GPCho(38:y).

To examine lysoGPCho species, however, the dominating diacyl and alkylacyl/alkenylacyl GPCho species were excluded from a subsequent analysis by scanning for m/z 184 precursors in the mass range m/z 400-700. Peak analysis of the resultant short range spectra from BSF WT lipids revealed the following set of $[M+H]^+$ lipid metabolites: lysoGPCho(-/22:6), lysoGPCho(-/22:5), lysoGPCho(-/22:4), lysoGPCho(-/18:2), lysoGPCho(-/18:1), lysoGPCho(-/18:0), lysoGPCho(-/20:2), lysoGPCho(-/20:3), and lysoGPCho(-/20:4). The peaks representing these metabolites and their $[M+H]^+$ value are shown (Fig. 3B, panel 1).

Qualitative comparison of the BSF lysoGPCho spectrum peaks with those from PCF analysis indicated that their abundance was significantly increased in the BSF spectra. To further investigate this result the lysoGPCho series metabolites were quantitated by comparison to non-natural lysoGPCho(17:0/-) and lysoGPCho(24:0/-) added to each sample prior to lipid extraction (Fig. 3B, panel 1 inset). From these quantitative ESI-MS-MS experiments it was perceived that BSF WT cells possessed 3-fold the number of moles of total lysoGPCho than in PCF WT cells (Table 1). However, this lysoGPCho increase was not distributed evenly among the major lysoGPCho series. There was a 3.9-fold increase in the lysoGPCho(-/22:y) series whereas only a 1.3-fold increase was observed in the lysoGPCho(-/20:y) series. It is, however, important to recall that an observed increase or decrease in a lysoGPCho metabolite doesn't

necessarily equate to its increased or decreased rate of synthesis; the change could be accounted for by an increase or decrease in the rate at which these intermediates are further metabolized.

The synthesis of lysoGPCho molecules in BSF *T. brucei* are mediated by TbPLA₁ since *Δpla1* cells show a very significant drop in their levels (Fig. 3B, panel 2). The number of moles of lysoGPCho in BSF *Δpla1* null mutants was recorded to be roughly 20% of those metabolite levels in WT cells (Table 1) (Fig. 3B, panel 2 inset). The individual lysoGPCho(-/18:y), lysoGPCho(-/20:y) and lysoGPCho(-/22:y) series levels decreased by 77%, 60%, and 84% in the BSF *TbPLA₁* null mutants, respectively. This decline in the ability to synthesize lysoGPCho was confirmed to be the direct result of the loss of *TbPLA₁* since tetracycline-induced *Δpla1 rescPLA1-HA* cells rescued lysoGPCho synthesis (Fig. 3B, panels 3 and 4). This recovery is only modest due to the small amount of PLA1-HA synthesized from over-expressed *PLA1-HA* mRNA (Fig. 2C). The individual lysoGPCho(-/18:y), lysoGPCho(-/20:y) and lysoGPCho(-/22:y) series levels were restored to 41%, 73%, and 46% of normal BSF levels of these metabolites in these cells, respectively (Fig. 3B, panels 3 and 4 and their respective insets) (Table 1).

TbPLA₁ null mutants still possess a small amount of lysoGPCho. There are several explanations for this observation. It is possible that an alternative phospholipase, or more, is responsible for a low level of synthesis *in vivo*. However, lysates of PCF *Δpla1* cells could no longer produce any lysoGPCho in an *in vitro* assay [4], and this is also true for BSF *Δpla1* cells (data not shown). Much of the lysoGPCho peak area in *Δpla1* cells could be contributed by background levels of fragment ions mechanically formed from diacyl GPCho during the sample preparation and/or the ionization process. Also, BSF *T. brucei* is known to efficiently uptake exogenous lysoGPCho from both culture and the host's bloodstream [18, 20]; therefore, some of the unsaturated lysoGPCho species present in *Δpla1* mutants could be from LDL-linked or albumin-linked unsaturated lysoGPCho from host plasma, the abundance of which is estimated to be 4.2 and 25.9 nmol/ml of human plasma, respectively [23].

Kinetic analysis of lysoGPCho synthesis

Both *in vivo* and *in vitro*, TbPLA₁ is a soluble enzyme that acts on insoluble lamellar GPCho substrates. In order to achieve lysoGPCho synthesis, therefore, TbPLA₁ must 1) adsorb to membrane surfaces, i.e. undergo interfacial activation, and 2) cleave the *sn*-1 ester of its substrate. The mechanism by which the latter is accomplished is through the action of a Ser-His-Asp catalytic triad [4]. The following experiments give insight into the mechanism of interfacial activation and binding properties of TbPLA₁.

Analytically, the actions of soluble lipolytic enzymes can be manifested by employing 'surface dilution' kinetics [28-30], and this can be applied to give insight into the mechanism by which an interfacial enzyme initially binds to an aggregate [32](see the 'Experimental' section for an explanation of this kinetic scheme). 'Surface dilution' kinetics for recombinant TbPLA₁ was carried out with the use of mixed micelles composed of GPCho(16:0/16:0), Bis-BODIPY[®] FL-C₁₁-PC, and TX-100. Surface dilution was accomplished by adding the nonionic detergent TX-100 in increments while keeping the substrate concentration constant. TbPLA₁ activity at various substrate surface concentrations (0.036, 0.018, and 0.009 mole fractions) was then measured as a function of various substrate bulk concentrations.

Firstly, an experiment was carried out to examine the possibility that the enzyme binds nonspecifically to the micelle surface, the 'surface binding' model. In this instance the aggregate molecules are expressed as the molar concentration of both the lipid and detergent that make up the aggregate. Comparison of TbPLA₁ activity at various surface concentrations shows that as the surface concentration of lipid decreases there is a decrease in the apparent V_{\max} , this is the surface dilution phenomenon (Fig. 4A). The true V_{\max} is the V_{\max} at an infinite mole fraction of PL substrate. The linear relationship between the decrease in activity as the surface concentration of substrate decreases also shows that TbPLA₁ doesn't have a strong affinity for individual TX-100 molecules, since they are in great excess over the substrate at all mole fractions.

Theoretical predictions of the 'surface binding' model state that in a double-reciprocal plot of Fig. 4A the lines should converge at a point where its *y*-axis ordinate represents $1/V_{\max}$ (Fig. 4B). The linear regression lines presented adequately converge, but kinetic constants were more easily obtained using the $1/v$ intercepts from Fig. 4B in a replot against the reciprocal of the mole fractions from which they were derived (Fig. 4C). The data from this plot produce a

straight line whose intercept of the $1/v$ intercept axis represents the true $1/V_{\max}$, and the $1/[\text{mole fraction}]$ intercept is the $-1/K_m$, where K_m is the interfacial Michaelis constant for the mixed micelle. The V_{\max} and K_m towards GPCho(16:0/16:0) were calculated to be 487 $\mu\text{mol}/\text{min}/\text{mg}$ and 0.22, respectively. The surface dilution kinetics equations also predict that if the kinetic model being employed is correct then a replot of the slopes of the lines in Fig. 4B versus the reciprocal of the mole fractions should be linear and pass through the origin, as seen in our replot (Fig. 4D). The data presented seem to fit the ‘surface binding’ model.

It is also feasible that the enzyme could specifically bind to a lipid substrate in the micelle with one binding domain, forming EA, prior to specifically binding to another lipid molecule for catalysis; this case has been termed the ‘dual phospholipid binding’ model [29, 30]. Analysis can be carried out according to this model using the same data used to test the first model [33]. Accordingly, a plot of PLA₁ activity as a function of the molar concentration of GPCho(16:0/16:0) shows again that the enzyme activity is dependent on surface concentration of substrate (Fig. 5A). The double reciprocal plot of the data in Fig. 5A show that the linear regression lines of the data do not converge as predicted in the ‘dual phospholipid binding’ model (Fig. 5B). A replot of the $1/v$ intercepts from the three data sets used in Fig. 5B versus the reciprocal of the mole fraction produces the same result as in Fig. 5C and the K_m and V_{\max} values are thus identical. A plot of the slopes in Fig. 5B versus the reciprocal of the mole fraction produces a straight line that doesn’t pass through the origin, which suggests that the data doesn’t fit the ‘dual phospholipid binding’ model.

Kinetic analysis thus seems to indicate that TbPLA₁ activation *in vitro* is mediated by binding non-specifically to the mixed micelle interface prior to binding and catalyzing a PL substrate. The use of TX-100/GPCho(16:0/16:0)/Bis-BODIPY[®] FL-C₁₁-PC mixed micelles in a 96-well plate assay to perform kinetics greatly facilitated experimental procedure and improves upon some drawbacks experienced in previously used assay methods which were more laborious, lacked sensitivity [28], and/or used unnatural thiol ester substrate analogs which are poor substrates compared to oxyester lipids [29, 34].

Evidence for EA formation

The kinetic studies provided fundamental insight into the mechanism of activation of recombinant TbPLA₁, but making a conclusion that interfacial activation is substrate independent could not be made until verified independently. If the first kinetic model is accurate, TbPLA₁ should be able to bind to an aggregate whose surface is devoid of PL substrate and composed solely of nonionic diluters. To test this prediction, a Superdex 200 size exclusion column equilibrated in the presence or absence of lipid-free TX-100 micelles was loaded with a solution containing purified recombinant TbPLA₁. The sample was spiked with RNase A as an internal standard and the elution absorbance was monitored at UV₂₈₀ nm. In the absence of an interface, the majority of TbPLA₁ was shown by peak area analysis to elute in monomer form (38.7 kDa, 96%); whereas a small proportion of enzyme eluted in the void volume and as a 'dimer' (75.9 kDa) (Fig. 6).

In contrast, the affinity of recombinant TbPLA₁ for a pure TX-100 micelle surface is demonstrated by a shift in its elution time from 29.7 to 25.8 min., representing an increase in apparent molecular weight from 38.7 kDa to 134 kDa, respectively (Fig. 6). This increase of 95.3 kDa corresponds very well to an increase in molecular weight if a monomer of enzyme were bound to exactly one micelle of TX-100, which has a molecular weight of approximately 90 kDa [35].

These results provide evidence for enzyme-aggregate formation and are a testament to the non-specific adsorption mechanism employed by this enzyme during interfacial activation onto mixed micelles. This association to the micelle surface is not dependent on surface charge since TX-100 is non-ionic, and it is also not due to specific binding to TX-100 molecules (Fig. 4A). The non-specific nature of binding to TX-100 mixed micelles for TbPLA₁ contrasts with the nature of binding for cytosolic PA-PLA₁ partially purified from bovine testis, which requires anionic phosphoglycerides to bind to surfaces [36]. No other PLA₁s have been examined for their binding properties.

Metal ion effects on lysoGPCho formation

To more precisely understand the fundamental basis behind lysoGPCho formation by TbPLA₁, its biochemical properties and activity were further examined *in vitro*. Besides a requisite of

an interface for activation, some phospholipases require co-factors for optimal activity whereas others do not. For example, cytosolic PLA₂ activity is calcium-dependent; whereas another PLA₂ group, iPLA₂, is calcium-independent [37]. Conversely, the heavier metals can be potent inhibitors of lipase activity [17, 38]. In this study, both the metal ion co-factor and inhibitory profile for TbPLA₁ was assessed.

TbPLA₁ apparently has no absolute metal ion requirements for activity since prior dialysis or incubation of the enzyme with EDTA prior to commencing the reaction did not abolish lysoGPCCho synthesis (Table 2). This result is consistent with a previous finding that PLA₁ activity in lysates of *T. brucei* is divalent cation independent [39]. Also, magnesium and manganese did not enhance or alter TbPLA₁ activity as has been observed previously for mammalian PLA₁ [40]. On the other hand, a number of heavy metals inhibited TbPLA₁ activity at various concentrations, a phenomenon that has been observed before for PLA₁ activity in soluble fractions of *T. brucei* incubated with 5 mM metal ions [41]. The most potent metals are cadmium and copper, whose inhibitory effects can be observed at concentrations as low as 2 µM (Table 2). Incubation with different levels of iron produced partial to total inhibition whilst moderate inhibition was detected in the presence of relatively high concentrations of nickel and zinc. The inhibitory effects to TbPLA₁ *in vitro* upon pre-incubation with heavy metals are mediated by an undefined mechanism.

Effects of serine inhibitors on TbPLA₁ activity

Knowing that Ser-131 is the active site residue for TbPLA₁ [4], the next line of experiments sought to inhibit enzyme activity with the known active-site serine modifiers diisopropyl fluorophosphate (DFP), phenylmethylsulphonylfluoride (PMSF), and diethyl-*p*-nitrophenyl phosphate (E-600). It was anticipated that DFP would have little effect on PLA₁ activity originating from *T. brucei* [41]. Palmitoyl and arachidonyl trifluoromethyl ketone analogues (PACOCF₃ and AACOCF₃, respectively) were also examined for potential effects of product inhibition, as observed for cytosolic PLA₂ enzymes when in the presence of these compounds [42]. However, pre-incubation with moderate levels of all of these individual compounds with TbPLA₁ resulted in no inhibition, and only relatively little inhibition of PLA₁ activity was observed with a very high concentration of inhibitor (Table 3). These inhibitors covalently and

permanently modify accessible serine residues, and upon successful modification a complete loss of activity would be anticipated. The fact that TbPLA₁ is insensitive to working concentrations of these serine-modifying reagents suggests that the serine active site residue of TbPLA₁ is inaccessible. Many prokaryotic and eukaryotic lipases, which structurally have single and multiple domains, respectively, contain active sites buried within the enzyme that are sheltered by an α -helical lid structure, rendering the catalytic triad un-solvated [43, 44]. The active site of a lipase is able to cleave the substrate only after interfacial activation, and the α -helical lid structure plays a role in this enzyme activation [45]. In light of the failure of serine-modifying reagents to inhibit TbPLA₁, these results suggest that the active site of TbPLA₁ may also be covered by a similar lid structure when the enzyme is not adsorbed to membrane surfaces, and that interfacial activation of TbPLA₁ engenders a conformational change to expose these otherwise inaccessible active site elements that are needed for PL hydrolysis, a structural change that may be similar to lipase activation. Structural studies are underway to clarify this issue.

Conclusions

TbPLA₁ is constitutively expressed in both PCF and BSF trypanosomes. A reverse genetics approach was employed to study the effects of *TbPLA₁* deletion in BSF parasites. Ablation of TbPLA₁ resulted in a very drastic reduction of all the molecular species of lysoGPCho metabolites that were present in WT cells. Interestingly, despite the adoption and adaptation of *TbPLA₁* in the PCF life cycle stage [4], lysoGPCho levels in the BSF stage are 3-fold greater than in the PCF stage. *TbPLA₁* appears not to be essential for cell viability in culture nor for virulence in a mammalian host. Evidence that the enzyme is insensitive to serine-modifying reagents suggests that the catalytic triad active site of TbPLA₁ is buried inside the enzyme and sheltered by a lid domain, a property shared with other lipases. Furthermore, in a GPCho/TX-100 mixed micelle system this soluble, monomeric enzyme appears to adsorb to lipid/micelle interfaces non-specifically instead of requiring lipid substrates to achieve interfacial activation. On balance, the results suggest that this binding and activation mechanism could help to induce a favorable conformational change suspected to be needed to expose active site elements.

ACKNOWLEDGEMENTS

This work was supported by Wellcome Trust Senior Fellowship Grant 067441 and a Wellcome Trust Prize Studentship (to G.S.R.).

REFERENCES

- 1 Webb, H., Carnall, N., Vanhamme, L., Rolin, S., Van Den Abbeele, J., Welburn, S., Pays, E. and Carrington, M. (1997) The GPI-phospholipase C of *Trypanosoma brucei* is nonessential but influences parasitemia in mice. *J Cell Biol* **139**, 103-114.
- 2 Carrington, M., Carnall, N., Crow, M. S., Gaud, A., Redpath, M. B., Wasunna, C. L. and Webb, H. (1998) The properties and function of the glycosylphosphatidylinositol-phospholipase C in *Trypanosoma brucei*. *Mol Biochem Parasitol* **91**, 153-164.
- 3 Gruszyński, A. E., van Deursen, F. J., Albareda, M. C., Best, A., Chaudhary, K., Cliffe, L. J., del Rio, L., Dunn, J. D., Ellis, L., Evans, K. J., Figueiredo, J. M., Malmquist, N. A., Omosun, Y., Palenchar, J. B., Prickett, S., Punkosdy, G. A., van Dooren, G., Wang, Q., Menon, A. K., Matthews, K. R. and Bangs, J. D. (2006) Regulation of surface coat exchange by differentiating African trypanosomes. *Mol Biochem Parasitol* **147**, 211-223
- 4 Richmond, G. S. and Smith, T. K. (2007) A novel phospholipase from *Trypanosoma brucei*. *Mol Microbiol* **63**, 1078-1095
- 5 Givskov, M. and Molin, S. (1992) Expression of extracellular phospholipase from *Serratia liquefaciens* is growth-phase-dependent, catabolite-repressed and regulated by anaerobiosis. *Mol Microbiol* **6**, 1363-1374
- 6 Schmiel, D. H., Wagar, E., Karamanou, L., Weeks, D. and Miller, V. L. (1998) Phospholipase A of *Yersinia enterocolitica* contributes to pathogenesis in a mouse model. *Infect Immun* **66**, 3941-3951
- 7 Dixon, H. and Williamson, J. (1970) The lipid composition of blood and culture forms of *Trypanosoma lewisi* and *Trypanosoma rhodesiense* compared with that of their environment. *Comp Biochem Physiol* **33**, 111-128
- 8 Patnaik, P. K., Field, M. C., Menon, A. K., Cross, G. A., Yee, M. C. and Butikofer, P. (1993) Molecular species analysis of phospholipids from *Trypanosoma brucei* bloodstream and procyclic forms. *Mol Biochem Parasitol* **58**, 97-105.
- 9 Balsinde, J. (2002) Roles of various phospholipases A2 in providing lysophospholipid acceptors for fatty acid phospholipid incorporation and remodelling. *Biochem J* **364**, 695-702.
- 10 Subbaiah, P. V., Liu, M., Bolan, P. J. and Paltauf, F. (1992) Altered positional specificity of human plasma lecithin-cholesterol acyltransferase in the presence of sn-2 arachidonoyl phosphatidyl cholines. Mechanism of formation of saturated cholesteryl esters. *Biochim Biophys Acta* **1128**, 83-92
- 11 McDermott, M., Wakelam, M. J. and Morris, A. J. (2004) Phospholipase D. *Biochem Cell Biol* **82**, 225-253
- 12 Fyrst, H., Oskouian, B., Kuypers, F. A. and Saba, J. D. (1999) The PLB2 gene of *Saccharomyces cerevisiae* confers resistance to lysophosphatidylcholine and encodes a phospholipase B/lysophospholipase. *Biochemistry* **38**, 5864-5871
- 13 Lee, K. S., Patton, J. L., Fido, M., Hines, L. K., Kohlwein, S. D., Paltauf, F., Henry, S. A. and Levin, D. E. (1994) The *Saccharomyces cerevisiae* PLB1 gene encodes a protein required for lysophospholipase and phospholipase B activity. *J Biol Chem* **269**, 19725-19730
- 14 Zaccheo, O., Dinsdale, D., Meacock, P. A. and Glynn, P. (2004) Neuropathy target esterase and its yeast homologue degrade phosphatidylcholine to glycerophosphocholine in living cells. *J Biol Chem* **279**, 24024-24033

- 15 Murray, J. P. and McMaster, C. R. (2005) Nte1p-mediated deacylation of
phosphatidylcholine functionally interacts with Sec14p. *J Biol Chem* **280**, 8544-8552
- 16 Howe, A. G. and McMaster, C. R. (2006) Regulation of phosphatidylcholine
homeostasis by Sec14. *Can J Physiol Pharmacol* **84**, 29-38
- 17 Ridgley, E. L. and Ruben, L. (2001) Phospholipase from *Trypanosoma brucei* releases
arachidonic acid by sequential sn-1, sn-2 deacylation of phospholipids. *Mol Biochem
Parasitol* **114**, 29-40.
- 18 Bowes, A. E., Samad, A. H., Jiang, P., Weaver, B. and Mellors, A. (1993) The
acquisition of lysophosphatidylcholine by African trypanosomes. *J Biol Chem* **268**,
13885-13892.
- 19 Samad, A., Licht, B., Stalmach, M. E. and Mellors, A. (1988) Metabolism of
phospholipids and lysophospholipids by *Trypanosoma brucei*. *Mol Biochem Parasitol*
29, 159-169.
- 20 Werbovetz, K. A. and Englund, P. T. (1996) Lipid metabolism in *Trypanosoma brucei*:
utilization of myristate and myristoyllysophosphatidylcholine for myristoylation of
glycosyl phosphatidylinositols. *Biochem J* **318**, 575-581.
- 21 Tizard, I. R., Nielsen, K., Mellors, A. and Assoku, R. K. (1977) Free fatty acids,
lysophospholipases, and the pathogenesis of African trypanosomiasis. *Lancet* **2**, 91.
- 22 Coppens, I., Levade, T. and Courtoy, P. J. (1995) Host plasma low density lipoprotein
particles as an essential source of lipids for the bloodstream forms of *Trypanosoma
brucei*. *J Biol Chem* **270**, 5736-5741.
- 23 Croset, M., Brossard, N., Polette, A. and Lagarde, M. (2000) Characterization of
plasma unsaturated lysophosphatidylcholines in human and rat. *Biochem J* **345 Pt 1**,
61-67
- 24 Sekas, G., Patton, G. M., Lincoln, E. C. and Robins, S. J. (1985) Origin of plasma
lysophosphatidylcholine: evidence for direct hepatic secretion in the rat. *J Lab Clin
Med* **105**, 190-194
- 25 Mellors, A. and Samad, A. (1989) The acquisition of lipids by African trypanosomes.
Parasitol Today **5**, 239-244
- 26 Wirtz, E., Hartmann, C. and Clayton, C. (1994) Gene expression mediated by
bacteriophage T3 and T7 RNA polymerases in transgenic trypanosomes. *Nucleic Acids
Res* **22**, 3887-3894
- 27 Bligh, E. G. and Dyer, W. J. (1959) A rapid method of total lipid extraction and
purification. *Can J Biochem Physiol* **37**, 911-917
- 28 Deems, R. A., Eaton, B. R. and Dennis, E. A. (1975) Kinetic analysis of phospholipase
A2 activity toward mixed micelles and its implications for the study of lipolytic
enzymes. *J Biol Chem* **250**, 9013-9020
- 29 Hendrickson, H. S. and Dennis, E. A. (1984) Kinetic analysis of the dual phospholipid
model for phospholipase A2 action. *J Biol Chem* **259**, 5734-5739.
- 30 Roberts, M. F., Deems, R. A. and Dennis, E. A. (1977) Dual role of interfacial
phospholipid in phospholipase A2 catalysis. *Proc Natl Acad Sci U S A* **74**, 1950-1954
- 31 Wirtz, E., Leal, S., Ochatt, C. and Cross, G. A. (1999) A tightly regulated inducible
expression system for conditional gene knock-outs and dominant-negative genetics in
Trypanosoma brucei. *Mol Biochem Parasitol* **99**, 89-101.
- 32 Carman, G. M., Deems, R. A. and Dennis, E. A. (1995) Lipid signaling enzymes and
surface dilution kinetics. *J Biol Chem* **270**, 18711-18714

- 33 Buxeda, R. J., Nickels, J. T., Jr., Belunis, C. J. and Carman, G. M. (1991) Phosphatidylinositol 4-kinase from *Saccharomyces cerevisiae*. Kinetic analysis using Triton X-100/phosphatidylinositol-mixed micelles. *J Biol Chem* **266**, 13859-13865
- 34 Kucera, G. L., Miller, C., Sisson, P. J., Wilcox, R. W., Wiemer, Z. and Waite, M. (1988) Hydrolysis of thioester analogs by rat liver phospholipase A1. *J Biol Chem* **263**, 12964-12969.
- 35 Helenius, A., McCaslin, D. R., Fries, E. and Tanford, C. (1979) Properties of detergents. *Methods Enzymol* **56**, 734-749
- 36 Lin, Q., Higgs, H. N. and Glomset, J. A. (2000) Membrane lipids have multiple effects on interfacial catalysis by a phosphatidic acid-preferring phospholipase A1 from bovine testis. *Biochemistry* **39**, 9335-9344
- 37 Six, D. A. and Dennis, E. A. (2000) The expanding superfamily of phospholipase A(2) enzymes: classification and characterization. *Biochim Biophys Acta* **1488**, 1-19
- 38 Pete, M. J., Ross, A. H. and Exton, J. H. (1994) Purification and properties of phospholipase A1 from bovine brain. *J Biol Chem* **269**, 19494-19500.
- 39 Hambrey, P. N., Mellors, A. and Tizard, I. R. (1981) The phospholipases of pathogenic and non-pathogenic *Trypanosoma* species. *Mol Biochem Parasitol* **2**, 177-186.
- 40 Higgs, H. N. and Glomset, J. A. (1996) Purification and properties of a phosphatidic acid-preferring phospholipase A1 from bovine testis. Examination of the molecular basis of its activation. *J Biol Chem* **271**, 10874-10883
- 41 Opperdoes, F. R. and van Roy, J. (1982) The phospholipases of *Trypanosoma brucei* bloodstream forms and cultured procyclics. *Mol Biochem Parasitol* **5**, 309-319.
- 42 Wissing, D., Mouritzen, H., Egeblad, M., Poirier, G. G. and Jaattela, M. (1997) Involvement of caspase-dependent activation of cytosolic phospholipase A2 in tumor necrosis factor-induced apoptosis. *Proc Natl Acad Sci U S A* **94**, 5073-5077
- 43 Jaeger, K. E., Ransac, S., Dijkstra, B. W., Colson, C., van Heuvel, M. and Misset, O. (1994) Bacterial lipases. *FEMS Microbiol Rev* **15**, 29-63
- 44 Wong, H. and Schotz, M. C. (2002) The lipase gene family. *J Lipid Res* **43**, 993-999.
- 45 Winkler, F. K., D'Arcy, A. and Hunziker, W. (1990) Structure of human pancreatic lipase. *Nature* **343**, 771-774

FIGURE LEGENDS

Figure 1 *TbPLA₁* expression profile

(A) Northern blot analysis of BSF and PCF WT total RNA (12 µg) probed with the *TbPLA₁* ORF (top panel). Constitutive expression is revealed by the detection of a single band from both lanes. Loading was controlled for by re-probing the blot with the β -tubulin ORF (bottom panel). (B) Western blot analysis of 10⁷ BSF and PCF WT cell equivalents. *TbPLA₁* was detected using antibodies raised against the recombinant protein. * = non-related background band to show loading control.

Figure 2 Validation of the generation of *TbPLA₁* Mutants

(A) *TbPLA₁* null mutants were generated in BSF *T. brucei* after sequential *TbPLA₁* UTR targeted homologous recombination with UTR-flanked puromycin and hygromycin resistance genes. Cell lines were analyzed by Southern blot after digesting genomic DNA with *AlwI*, which cuts *TbPLA₁* internally. *AlwI* digested *T. brucei* WT DNA therefore reveals two fragments detectable by fluorescein-labeled *TbPLA₁* ORF probe. In the three *TbPLA₁* null mutant cell lines (Δ *pla1*) both *TbPLA₁* alleles are absent. A tetracycline (Tet) inducible HA-tagged recombinant ectopic copy of *TbPLA₁* (*PLA1-HA*) in *pLEW82/PLA1-HA* was introduced into a different locus in the Δ *pla1* cell line to produce a rescue cell line (Δ *pla1 rescPLA1-HA*). (B) Northern blot analysis of *TbPLA₁* mutants. Total RNA extracted from BSF WT and *TbPLA₁* mutant trypanosomes was resolved by electrophoresis, transferred to nitrocellulose, and hybridized with the ORF of *TbPLA₁* (top panel), a β -tubulin hybridization was used as a loading control (bottom panel). (C) Western blot analysis of *TbPLA₁* mutants (10⁷ cell equivalents/lane). Both native *PLA₁* (theoretically 32.4 kDa) and tagged *PLA₁-HA* (theoretically 33.8 kDa) protein were separated on a 15% SDS-PAGE gel and detected by antibodies raised against the purified recombinant enzyme. (D) *In vitro* growth analysis of BSF *TbPLA₁* mutants. The logarithmic cumulative growth of the WT, null mutant and rescue cell lines is plotted as a function of culture duration. The population growth was calculated as cell density multiplied by the cumulative dilution factors obtained from daily passaging of the cells. * = non-related background bands that show loading in the null mutant lanes.

Figure 3 *TbPLA₁*-mediated lysoGPCho synthesis in BSF *T. brucei*

(A) GPCho composition of *T. brucei* BSF WT cells spiked with the internal standards lysoGPCho(-/17:0) and lysoGPCho(-/24:0). The spectrum was acquired from positive ion ESI-MS-MS precursor ion scanning for m/z 184 ions. Identities of the major $[M+H]^+$ ions are indicated. (B) Short-range ESI-MS-MS spectra in positive ion mode showing the parents of the m/z 184 ion from total lipid extracts from WT and *TbPLA₁* mutant cell lines. The lysoGPCho $[M+H]^+$ metabolites detected are boxed and annotated next to the m/z peak from which they derived. x:y refers to the total number of *sn*-2 FA carbon atoms (x) and their degree of unsaturation (y). Panel insets show short-range spectra from lipid extracts from each cell line that were spiked with lysoGPCho internal standards.

Figure 4 *TbPLA₁* activity in relation to the ‘surface binding’ model

(A) the fluorescent BODIPY[®]C₁₁-PC assay was used to rate PLA₁ velocity (V) as a function of varying bulk concentrations of GPCho(16:0/16:0) plus TX-100 at set mole fractions (X_s). The data points shown are the average from three separate experiments each performed in triplicate. The data points varied by less than one standard deviation, the overlapping ranges have been omitted for clarity. (B) reciprocal plot of the data in panel A. (C) replot of the 1/V intercepts from panel B versus the reciprocal of the mole fraction. (D) replot using the slopes obtained in panel B versus the reciprocal of the mole fraction from which they were derived. The lines drawn in panels B, C, and D were fitted to the data after linear regression analysis.

Figure 5 *TbPLA₁* activity in relation to the ‘dual phospholipid binding’ model

(A) the fluorescent BODIPY[®]C₁₁-PC assay was used to rate PLA₁ velocity (V) as a function of varying only bulk concentrations of GPCho(16:0/16:0) at set mole fractions (X_s). The data points shown are the average from three separate experiments each performed in triplicate. The data points varied by less than one standard deviation, the overlapping ranges have been omitted for clarity. (B), (C), and (D), same as in Fig. 4.

Figure 6 Adsorption of *TbPLA₁* onto detergent micelles

Size exclusion chromatography elution profiles of a sample of recombinant *TbPLA₁* (1.25 mg) spiked with an RNase A internal standard (13.7 kDa) are plotted as a function of their UV

absorbance at 280 nm (A_{280}). The peak elution times of TbPLA₁ in the absence (29.7 min.) or presence (25.8 min.) of TX-100 micelles were compared to the molecular weight standard elution times (shown above the top *x-axis*) in order to calculate an approximate molecular weight shift (see 'Experimental'). The RNase A internal standard (35.9 min.) and void volume (16 min.) peaks displayed equivalent elution times in both buffers. Peak identities were confirmed using SDS-PAGE of the eluate fractions (data not shown).

Table 1 Quantitation of lysoGPCho in WT and BSF *TbPLA_I* mutants

The lysoGPCho content of lipid extracts from 10^8 *T. brucei* cells was measured with lysoGPCho(17:0/-) and lysoGPCho(24:0/-) as internal standards. Values are from a typical analysis and are presented as pmol/ 10^8 cells. Tet = tetracycline, * = Integration of m/z $[M+H]^+$ signals to obtain peak areas was performed by assembling individual lysoGPCho into a series of peaks whereby one series comprises both the major and minor lysoGPCho molecules, and their isotopes, containing the same fatty acid chain length but with varying degrees of unsaturation, represented by 'y'.

| Cell line | Tet | lysoGPCho series* (pmol/ 10^8 cells) | | | Total |
|--------------------------|-----|--|----------|----------|-------|
| | | (-/18:y) | (-/20:y) | (-/22:y) | |
| WT (PCF) | | 53 | 31 | 72 | 156 |
| WT (BSF) | | 143 | 40 | 280 | 463 |
| <i>Δp1a1</i> | | 33 | 16 | 45 | 94 |
| <i>Δp1a1 rescPLA1-HA</i> | - | 35 | 20 | 48 | 103 |
| <i>Δp1a1 rescPLA1-HA</i> | + | 59 | 29 | 128 | 216 |

Table 2 Phospholipase A₁ activity with various compounds

All compounds were pre-incubated with enzyme (400 pg) for 10 minutes at the listed concentrations before commencing the reaction by the addition of substrate to a final concentration of 0.075 mM. Activity was measured using the fluorescent BODIPY[®]C₁₁-PC assay at pH 7.0 for 32 minutes with a mole fraction of 0.018. Values presented are the percentage of activity observed relative to the enzyme-only control. Data are averages (with percent standard deviation) obtained from two experiments performed in duplicate. † = enzyme-only control set at 100% (26 μmol min⁻¹ mg⁻¹), ‡ = Maximum EDTA added was 10 mM, resulting in 91% relative activity, * = p < .05, ** = p < .005

| Additive | % Relative activity | | | |
|-------------------|---------------------|---------|---------|----------|
| | 2 μM | 20 μM | 200 μM | 2 mM |
| None [†] | 100 | 100 | 100 | 100 |
| MgCl ₂ | 98 (3) | 85 (9) | 94 (3) | 96 (2) |
| CaCl ₂ | 101 (2) | 91 (5) | 92 (10) | 87 (9) |
| MnCl ₂ | 97 (5) | 99 (2) | 104 (2) | 87 (6) |
| FeCl ₂ | 83 (4) | 76 (7) | 20 (2)* | 0 (0)** |
| CoCl ₂ | 99 (0) | 101 (0) | 90 (5) | 57 (2)* |
| NiCl ₂ | 102 (1) | 94 (3) | 85 (7) | 43 (10)* |
| CuCl ₂ | 55 (4)* | 6 (1)** | 0 (0)** | 0 (0)** |
| ZnSO ₄ | 105 (1) | 93 (4) | 59 (9)* | 34 (6)* |
| CsCl ₂ | 101 (2) | 112 (1) | 112 (0) | 102 (2) |
| CdCl ₂ | 81 (5) | 37 (8)* | 1 (1)** | 0 (0)** |
| EDTA [‡] | 98 (0) | 94 (4) | 91 (5) | 96 (2) |

Table 3 TbPLA₁ Activity in the Presence of Various Inhibitors

All inhibitors were pre-incubated with enzyme (600 pg) for 10 minutes at the listed concentrations and conditions before commencing the reaction by the addition of substrate to a final concentration of .075 mM. Activity was measured using the fluorescent BODIPY[®]C₁₁-PC assay at pH 7.0 for 32 minutes with a mole fraction of 0.018. Values presented are the percentage of activity observed relative to the enzyme-only control. Data are averages (with percent standard deviation) obtained from three experiments performed in triplicate. † = enzyme-only control set at 100% (38 μmol min⁻¹ mg⁻¹), * = p < .05.

| Serine modifier | % Relative activity | | |
|---------------------|---------------------|---------|---------|
| | 10 mM | 1 mM | 0.1 mM |
| None [†] | 100 | 100 | 100 |
| DFP | 79 (9)* | 104 (1) | 99 (0) |
| PMSF | - | 91 (6) | 95 (3) |
| E-600 | 72 (8)* | 89 (7) | 99 (3) |
| AACOCF ₃ | 87 (4)* | 99 (0) | 100 (1) |
| PACOCF ₃ | 61 (4)* | 98 (1) | 98 (3) |

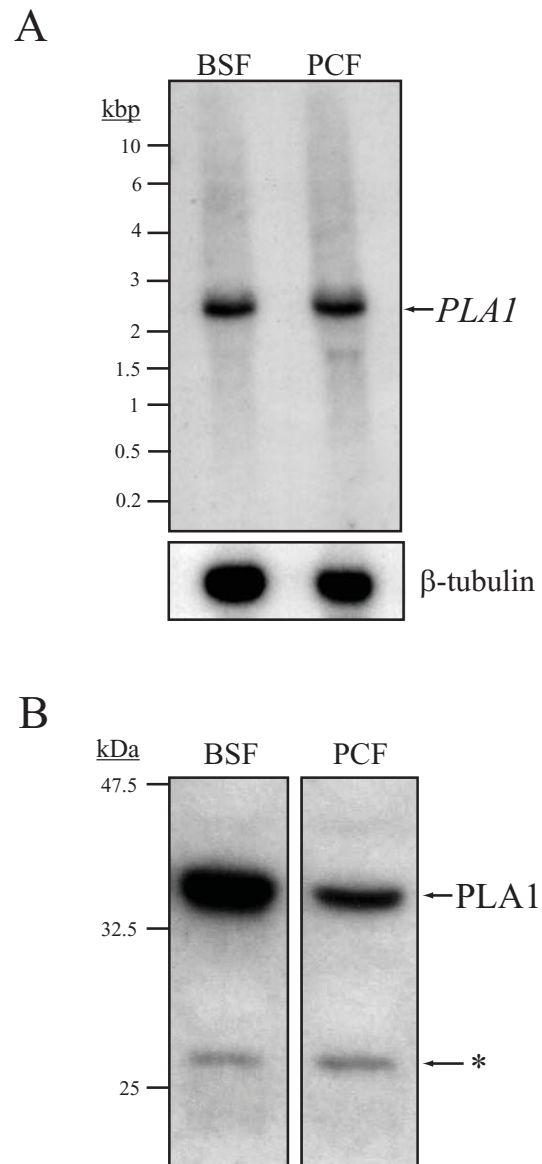


Figure 1

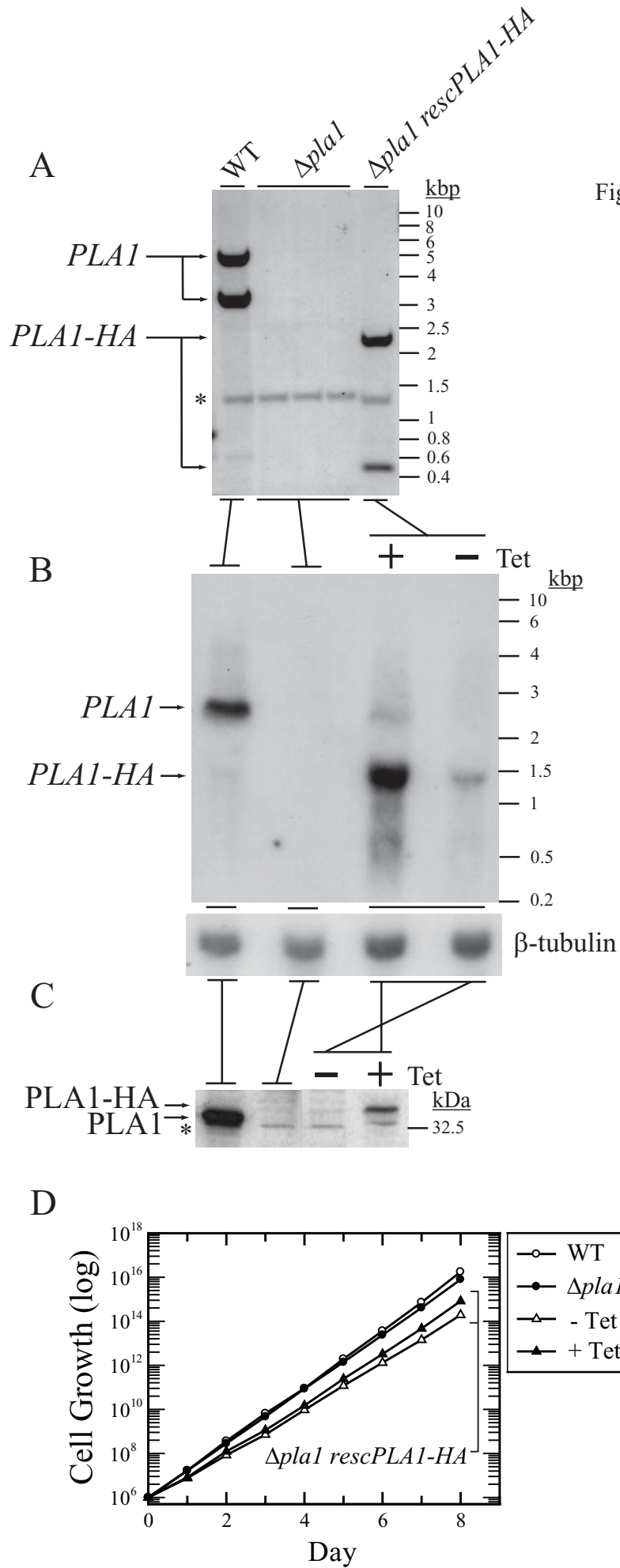
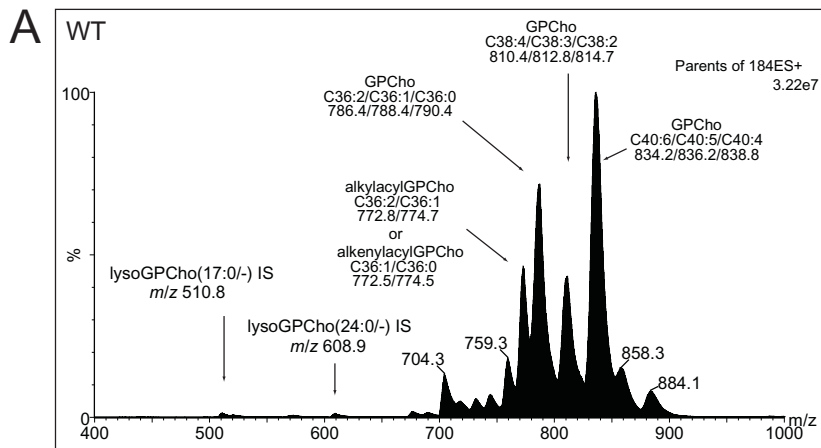
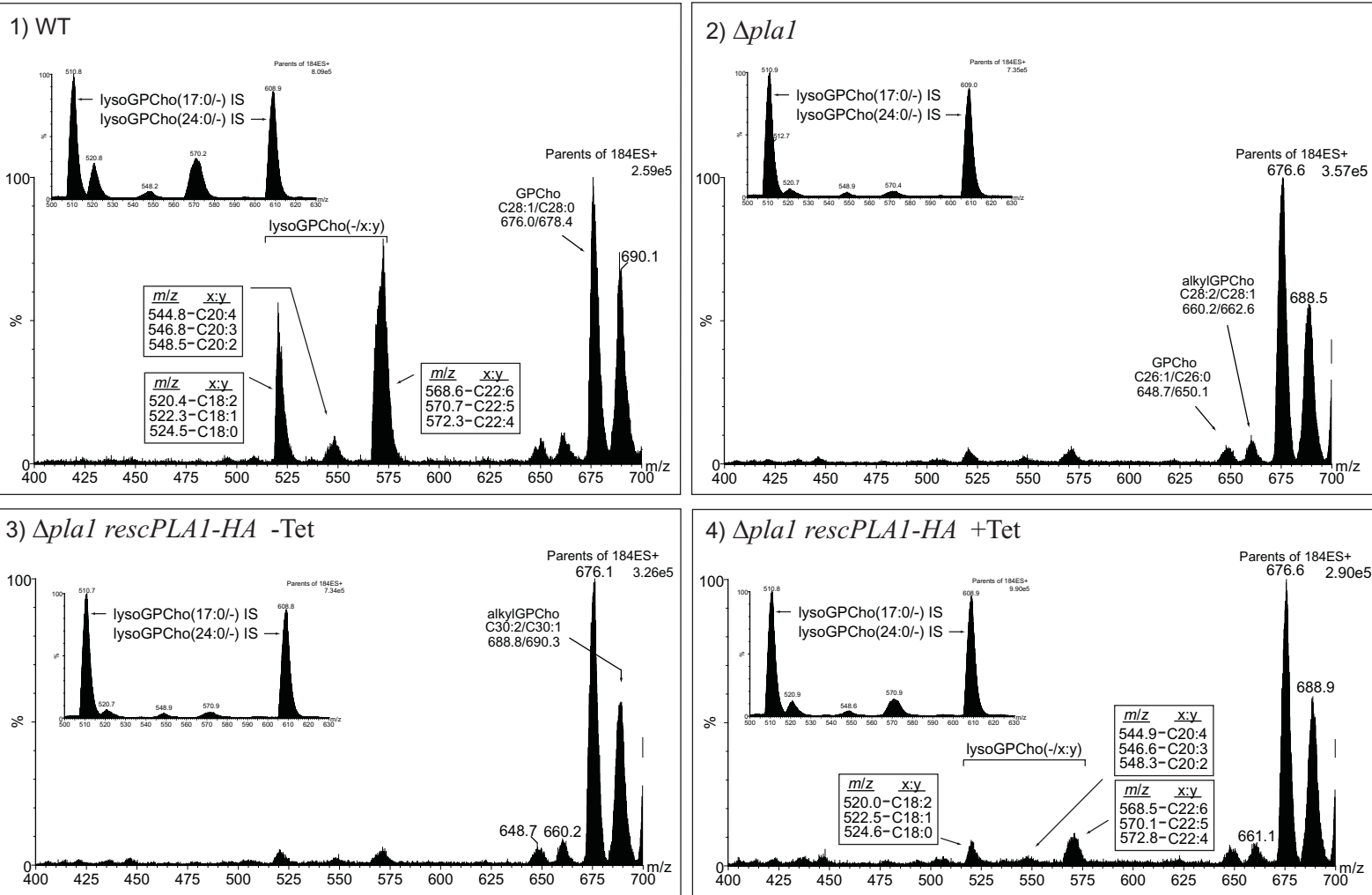


Figure 3



B



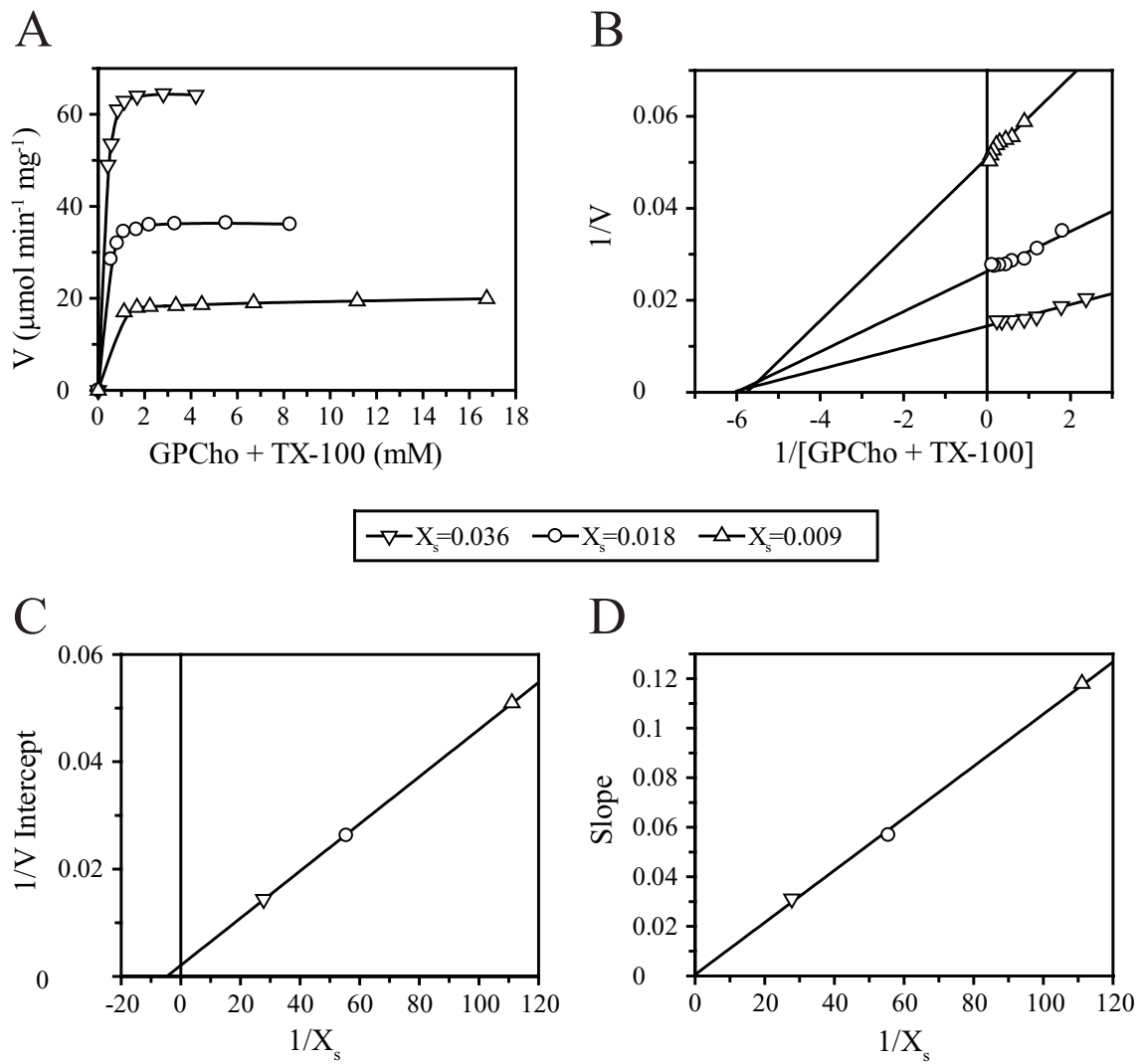


Figure 4

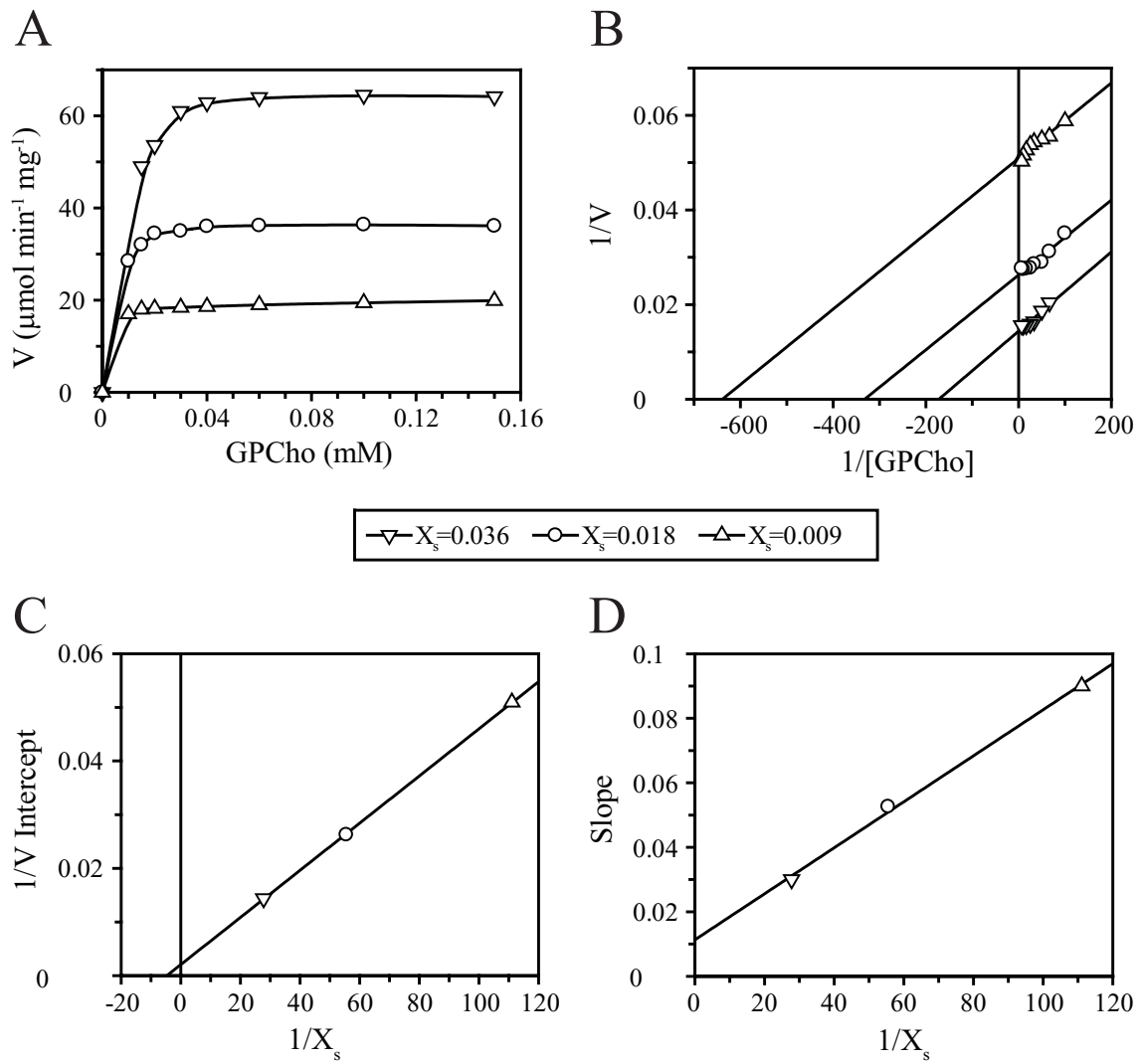


Figure 5

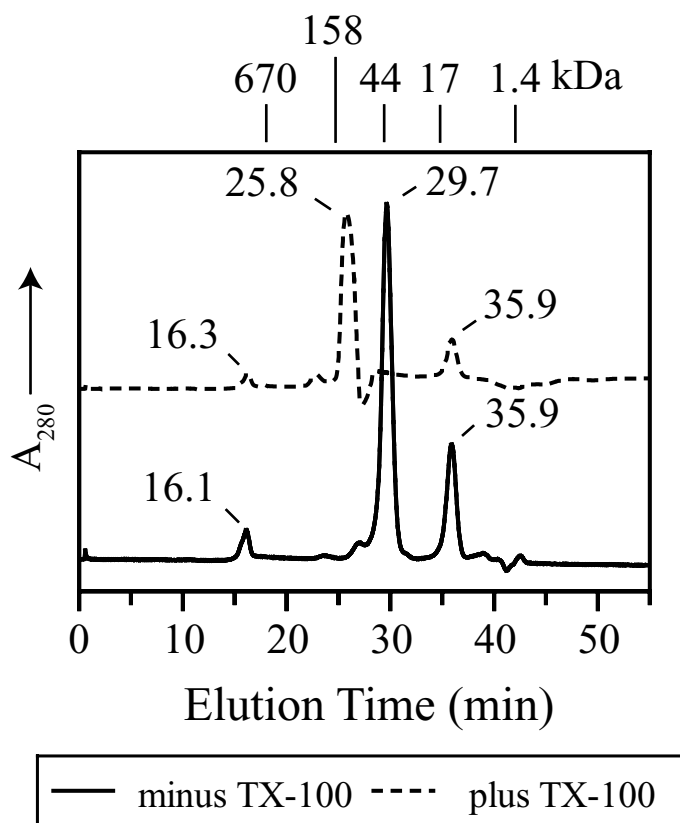


Figure 6